Biochimica et Biophysica Acta 1858 (2016) 38–46

Contents lists available at ScienceDirect

Biochimica et Biophysica Acta

journal homepage: www.elsevier.com/locate/bbamem

Molecular view of the interaction of S-methyl methanethiosulfonate with DPPC bilayer

Virginia Miguel [a], Maria E. Defonsi Lestard [b], María E. Tuttolomondo [b], Sonia B. Díaz [b], Aida Ben Altabef [b], Marcelo Puiatti [a,*], Adriana B. Pierini [a]

[a] INFIQC-CONICET, Instituto de Investigaciones en Físico-Química de Córdoba, Departamento de Química Orgánica, Facultad de Ciencias Químicas, Universidad Nacional de Córdoba, Ciudad Universitaria, X5000HUA Córdoba, Argentina

[b] INQUINOA-CONICET, Cátedra de Fisicoquímica I, Instituto de Química Física, Facultad de Bioquímica, Química y Farmacia, Universidad Nacional de Tucumán, San Lorenzo 456, T4000CAN S. M. de Tucumán, Argentina

ARTICLE INFO

Article history:
Received 4 May 2015
Received in revised form 7 October 2015
Accepted 13 October 2015
Available online 23 October 2015

Keywords:
Molecular dynamics
DPPC
S-methyl methanethiosulfonate
PMF

ABSTRACT

We present molecular dynamics (MD) simulation studies of the interaction of a chemo preventive and protective agent, S-methyl methanethiosulfonate (MMTS), with a model bilayer of 1,2-dipalmitoyl-*sn*-glycero-3-phosphocholine (DPPC). We analyzed and compared its diffusion mechanisms with the related molecule dimethyl sulfoxide (DMSO).

We obtained spatially resolved free energy profiles of MMTS partition into a DPPC bilayer in the liquid-crystalline phase through potential of mean force (PMF) calculations using an umbrella sampling technique. These profiles showed a minimum for MMTS close to the carbonyl region of DPPC. The location of MMTS molecules in the DPPC bilayer observed in the MD was confirmed by previous SERS studies [1]. We decomposed PMF profiles into entropic and enthalpic contributions. These results showed that the driving force for the partitioning of MMTS into the upper region of DPPC is driven by a favorable entropy change while partitioning into the acyl chains is driven by enthalpy. On the other hand, the partition of DMSO into the membrane is not favored, and is driven by entropy instead of enthalpy. Free diffusion MD simulations using all atom and coarse grained (CG) models of DPPC in presence of MMTS were used to analyze the effect of DPPC-MMTS interaction. Density profiles showed that MMTS locates preferentially in the carbonyl region, as expected according to the PMF profile and the experimental evidence. MMTS presented two differential effects over the packing of DPPC hydrocarbonate chains at low or at high molar ratios. An ordering effect was observed when a CG MMTS model was used. Finally, free diffusion MD and PMF decomposition for DMSO were used for comparison.

1. Introduction

One of the most important general functions of lipids is their role as constituents of cellular membranes. These membranes not only separate cells from the external environment, but also compartmentalize cells and provide a special milieu for many important biochemical processes [2]. Biomembranes constitute a very complex heterogeneous mixture with variable composition that exists as a dynamic structure. One of their most abundant constituents in animals and plants are phosphatidylcholine derivatives, reason by which these compounds are usually employed as experimental or theoretical models of lipid membranes [3].

Molecular dynamics (MD) simulations have been widely employed for the study of the interaction of small molecules [4], drugs of variable size [5], amino acids [6], peptides [7], and different solutes with phospholipid bilayers and biomembranes. This technique allows an atomic resolution description that should be complementary to other techniques such as X-ray diffraction, NMR, IR, SERS, etc. Three major types of force fields (FFs) are available for the study of lipid bilayers: coarse grained (CG), united atom (UA) and all atom (AA). AA FFs provide a better description of the system properties although they require higher computational resources, while UA and CG models allow longer simulation times and the analysis of larger systems, at expense of molecular detail. The most employed AA FFs for lipid simulations are CHARMM [8], Lipid14, the Amber lipid force field [9], and the Stockholm lipids (Slipids) [10]. These FFs are suited for simulations of lipid bilayers in the correct phase using the isothermal — isobaric ensemble (NPT), which is the appropriate ensemble for studying the insertions of solutes into the bilayer. Slipids and Lipid14 are compatible with the General Amber FF (GAFF) [11] usually employed for simulating organic compounds, such us hormones, drugs, and solvents, while the CHARMM force field can be used with the CGEN-FF force field.

In 1993 Nakamura et al. [12] isolated S-methyl methanethiosulfonate (MMTS) (Scheme 1) from cauliflower, *Brassica oleracea L. var. Botrytis*, and found it to inhibit the UV-induced mutation in *Escherichia coli*. In

* Corresponding author.
E-mail address: mpuiatti@fcq.unc.edu.ar (M. Puiatti).

http://dx.doi.org/10.1016/j.bbamem.2015.10.008
0005-2736/

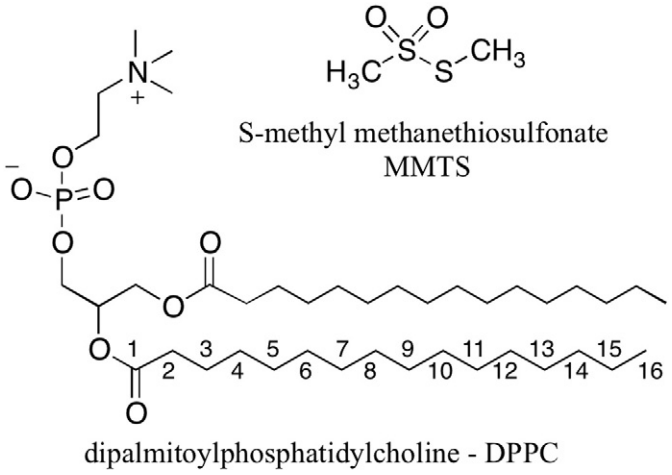

Scheme 1. MMTS and DPPC chemical structures.

1997 Sugie et al. [13] examined the modifying effect of MMTS on large bowel carcinogenesis and discovered that this organosulfur compound has a strong protective effect and suggested that MMTS is a promising chemo preventive agent for human liver neoplasms. Furthermore, its antioxidant activity against lipid peroxidation of MMTS was confirmed in tests with rabbit erythrocyte membrane ghosts or rat hepatocytes. [12] MMTS, present a preserving effect that could be related to a temperature shift in the fluid-to-gel transition temperature [1]. Results obtained by FTIR showed an increase in the DPPC transition temperature (from gel to liquid crystalline state) with increasing concentration of MMTS during the experiments [1].

Several co-solutes, as sugars [14], dimethyl sulfoxide (DMSO) [15], and alcohols [16] present the ability to affect the behavior of membranes inducing a temperature shift in the fluid-to-gel transition temperature. This shift is determined by the effect of the co-solute on the properties of the solvent (i.e. water) and/or the particular interactions that the cosolute can establish with the membrane [14a]. For the organic solvent DMSO that raises the fluid-to-gel transition temperature [16], it has been proposed that its action is caused by its preferential exclusion from the phosphatidyl bilayer, increasing the osmotic pressure of the bulk solvent over that of the interfacial region that results in a movement of water away from the interfacial zone stabilizing the gel phase [15a].

The main goal of the present work is to study the interaction of the promising chemo preventive and protective agent, MMTS, with a model bilayer of 1,2-dipalmitoyl-*sn*-glycero-3-phosphocholine (DPPC) by MD simulations. MMTS and DPPC are presented in Scheme 1. In particular, the interaction of MMTS with DPPC bilayers has been previously studied by a combination of Fourier transform infrared (FTIR) and Raman spectroscopy with quantum calculations, comparing the simulated and experimental FTIR and Raman spectra [1]. The energetic profiles for the insertion of MMTS in the bilayer were obtained from potential of mean force (PMF) calculations applying the umbrella sampling technique. In order to determine the molecular mechanism by which MMTS alters the properties of the membranes, we performed free diffusion MD simulations of lipid bilayers in presence of MMTS using AA and CG models. These results were contrasted with MD calculations of the partition of DMSO into DPPC in order to compare the diffusion mechanisms of these two related molecules.

2. Methods

2.1. Computational details

All simulations were carried out using the 4.6.3 Gromacs package with GPU acceleration [17]. The AA Slipids was used for lipids [18] and the TIP3P model [19] for water molecules. The starting geometries were obtained from Slipids on line resource [20]. Fully hydrated lipid bilayers (equilibrated at the mentioned temperatures) containing 128 l,2-dipalmitoyl-sn-glycero-3-phospcholine (DPPC) molecules were employed for equilibrium simulations.

The construction of MMTS unit to be used in MD simulations was achieved with the antechamber module, using the GAFF force field [11a], employing the restricted ESP (RESP) charges obtained from a single point HF/6–31G* [11b,21] quantum chemical calculation of the optimized structure (at B3LYP/6-31+G* level) within the Gaussian 03 package [22]. The parameters for DMSO were taken from the literature [23]. The AnteChamber PYthon Parser interfacE (ACPYPE) [24] was employed to change the format of the parameter files in order to use them with Gromacs code. The topology files with the parameters of the MMTS and DMSO units, atomic charges employed as well as the xyz coordinates of the optimized geometries are included in the supplementary material (SM). The molecular structure of MMTS has previously been determined in the gas phase from electron-diffraction data and by ab initio and density functional theory (DFT) calculations [25]. The geometry, force constants and torsional energy profiles reported by Tuttolomondo et al. were compared with the GAFF parameters used in this work and they are in good agreement (see Table S-1, and Fig. S-1).

The PMF simulations were carried out in a fully hydrated lipid DPPC bilayer containing 64 lipid molecules. Free energy profile calculations were derived from the PMF $\Delta G(z)$ calculation as a function of the distance of the MMTS to the bilayer center along the z-axis normal to the plane of the bilayer. A series of 20 separate simulations, of 20 ns each, were performed, in which the MMTS was restrained to a given depth in the bilayer by a harmonic restraint on the z-coordinate. A force constant of 1000 $kJ \cdot mol^{-1}\ nm^{-2}$ was used with a spacing of 0.2 nm between the centers of the biasing potentials. Two MMTS molecules were used, one per leaflet allowing error estimation. Finally, the Weighted Histogram Analysis Method (WHAM) was used to extract the PMF and calculate $\Delta\Delta G$ [26]. The error bars for these calculations were obtained using the bootstrap method [27].

The free energy can be decomposed into entropic and enthalpic components through its temperature dependence [28]. We performed the PMF and umbrella sampling calculations at three different temperatures (323, 338, and 353 K) and the entropic and enthalpic contributions to the free energy were evaluated using Eqs. (1) and (2) [28].

$$-T\Delta S = T\frac{\Delta G}{\Delta T} \approx \frac{T}{2\Delta T}(G(T+\Delta T) - G(T-\Delta T)) \quad (1)$$

$$\Delta H = \Delta G + T\Delta S \quad (2)$$

The PMFs at all three temperatures were aligned so they had a $\Delta\Delta G$ value of zero in the water phase (3.5 nm), and thus all free energies, enthalpies, entropies, and heat capacities are relative to the ones of MMTS in water.

For free diffusion MD, the simulation protocols were the same as in reference [18]. We used the MD parameters available in the Stockholm lipids' home page [29]. All bonds were constraint using Lincs algorithm. Constraining the bond lengths allowed a time step of 2 fs to be used. The Lennard–Jones interactions were truncated at 1.0 nm. The particle mesh Ewald method [30] was used to evaluate the electrostatic interactions, with a cutoff of 1.0 nm. The simulations were performed at an NPT ensemble. Four different concentrations of MMTS (~0.088 M, ~0.18 M; ~0.33 M, and ~0.44 M) were used for free diffusion simulations. These simulations systems were prepared as follows: 20, 40, 81 and 100 MMTS molecules were randomly located in the water solvent, respectively. The initial simulation boxes had similar dimensions in the bilayer plane (x–y) of (~64. 5 Å × ~65.7 Å) varying the height of the boxes being of 86.8 Å, 88.5 Å 95.6 Å, and 90.1 Å for the four systems in order to reach the desired concentrations. In the case of DMSO three concentrations were simulated (~0.18, ~0.36 M

and ~0.45 M) with 80 and 100 DMSO molecules in a box of ~88.2 Å in the *z*-axis. Prior to the MD production simulations (NPT ensemble), a minimization process of 3000 steps, and 100 ps of MD simulation at an NVT ensemble were ran, at a final temperature of 323 K. In these two processes the DPPC bilayer position was restrained. After the preparation steps, ~200 ns of MD simulations at 323 K within the NPT ensemble were collected for all the systems, the final 100 ns of these simulations were employed for the analysis of density profiles, deuterium order parameter, etc.

For CG simulations the BMW-MARTINI was selected since it consists of a model of water with three charge sites, and it reproduces the experimental dipole potential in membrane–water interface [31]. In BMW model four water molecules are mapped into one CG unit with three charge sites [31]. The protocol used for the CG parameterization of MMTS was the one proposed by MARTINI developers [32]. We use AA and CG membrane partitioning free energies of MMTS to check that our CG model reflects MMTS interaction with the bilayer (see SM Fig. S-2). We obtained a simplified model of MMTS that consist in two CG beads (C5 and Na) [33,31]. The C5 bead represents the nonpolar groups while Na bead is a hydrogen bond acceptor that represents the H-bonding atoms of MMTS (S = 0). As it can be observed in Fig. S-2, our two-beads MMTS CG model presents a very similar PMF profile of an AA model. With the parameterized model, we performed CG MMTS free diffusion MD simulations using a pre-equilibrated 128 DPPC lipid bilayer obtained from the BMW-Martini developers [34] in the presence of 96 MMTS molecules, [MMTS] = 0.42 M. We ran 600 ns MD simulations and analyzed the effect of MMTS onto DPPC bilayer. A MD simulation of a CG DPPC bilayer free of MMTS molecules was ran for 100 ns as a control. The order parameter was calculated using the do-order multi-4.py script downloaded from Martini home page [35].

This parameter is defined as:

$P2 = 0.5 * (3 * \cos^2\theta - 1)$.

where θ is the angle between the bond and the bilayer normal.

3. Results and discussion

This section is divided into four, free energy calculations using umbrella sampling MD, AA equilibrium MD simulations and CG free diffusion MD. In the first two sections, free energy calculations were used to describe the partition process of MMTS and DMSO into the bilayer, decomposing the ΔG profiles into their enthalpic and entropic(ΔH, and $-T\Delta S$) contributions. In the third section, different concentrations of MMTS were employed allowing the free diffusion of MMTS molecules into the DPPC bilayer in the liquid-crystalline state. Three simulations of DMSO at similar concentrations were also simulated to compare the net effect of both solutes over the DPPC bilayer. The results of free diffusion MD and PMF calculations of the partition of MMTS and DMSO into DPPC were used to analyze the diffusion mechanisms of these two related molecules. Finally, we performed CG MMTS free diffusion MD simulations in order to increase time sampling.

3.1. Calculation of the potential of mean force of MMTS–DPPC interaction

We performed PMF calculations to determine the probable distribution of MMTS and DMSO at different places of the lipidic system and to gain a thermodynamic insight of the process of their partition into the membrane. PMF was performed as a function of the distance to the center of the bilayer along its normal axis *z* [$\Delta G(z)$]. Free energy profile calculations were derived from the PMF extracted from a series of umbrella sampling simulations.

DPPC presents a main transition temperature or Tm at approx. 314 K [36]. MMTS potential of mean force calculations were performed for DPPC at liquid-crystalline (323 K) (Fig. 1) and at gel (298 K) phases (SM Fig. S-3). PMF curves were aligned so that the MMTS relative free energy in bulk water corresponds to zero in each case. The shapes of the free energy profiles are similar for both phases, two maxima in the

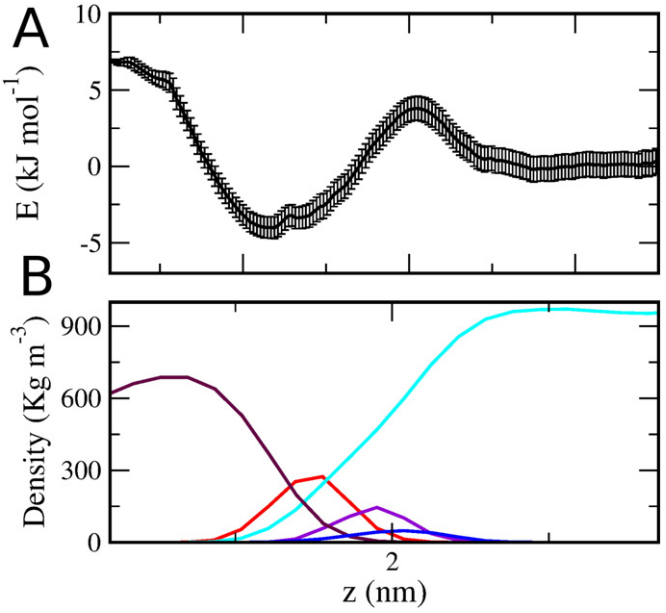

Fig. 1. MMTS free energy of partitioning into a DPPC bilayer. PMF of MMTS in a DPPC bilayer at liquid-crystalline phase. A) The upper panel displays the free energy (ΔG) 323 K. Error bars were obtained by bootstrap analysis using g_wham. B) Distribution of various chemical groups: choline (blue line); phosphate (violet line); carbonyls (red line), hydrocarbon chain (maroon line) and water (cyan line).

charged head group region (~2 nm) and center of the bilayer (0.5–0 nm) and the global minimum, which corresponds to the region of the carbonyl groups at 1–1.5 nm (Figs. 1-B and S-2B). The free energy change for transferring an MMTS molecule from water to the bilayer center was approx. 6.5 kJ·mol^{-1} (Fig. 1-A) with an initial barrier of ~4 kJ·mol^{-1} for crossing the polar head of the bilayer. The global energy minimum is approx. −4 kJ·mol^{-1}. It is important to remark that, according to the results obtained with PMF calculations, the most favored location of MMTS is within the carbonyl region of DPPC. Finally, the interaction of MMTS with the lipid charged head group is less favored than with the carbonyl, but stronger than with the hydrocarbon chain (Fig. 1).

Previous experimental FTIR results suggest intermolecular interactions between the head groups of DPPC and the CH_3 groups of MMTS [1]. The $\nu C=O$ peak in diacyl lipids can be decomposed in two components, H-bonded and non-bonded (free) population. In the gel and fluid state the $\nu C=O$ free populations increase, while in both states the $\nu C=O$ H-bonded population decrease, as MMTS concentration increase. These results indicated a water loss and H-bond formation with C=0 bonded population in the two phases [1]. This is in agreement with PMF calculations, were a minimum is located at the carbonyl region of diglyceride (Fig. 1-A).

3.2. Enthalpic and entropic decomposition of free energy calculation of MMTS and DMSO partition into DPPC bilayers

The mechanism by which MMTS works can be inferred from the interaction and the energies involved in its partition into the lipid membrane. The transfer of amphiphilic molecules from aqueous phase to lipid membrane can be caused by a system enthalpy lost (an exothermic process) and/or an entropy gain (an increment in system disorder). Free energy of transferring a molecule from bulk water to the membrane can be decomposed into these two components (entropic and enthalpic). To gain insight in the partitioning of MMTS into the bilayer, we obtained the spatially resolved entropic ($-T\Delta S$) and enthalpic (ΔH) component of free energy profile (Fig. 2A) based on umbrella sampling calculations at three different temperatures; 323, 338 and 353 K ($\Delta T = \pm 15$ K) (Fig. 2B). This approach has been applied before to both polar and apolar

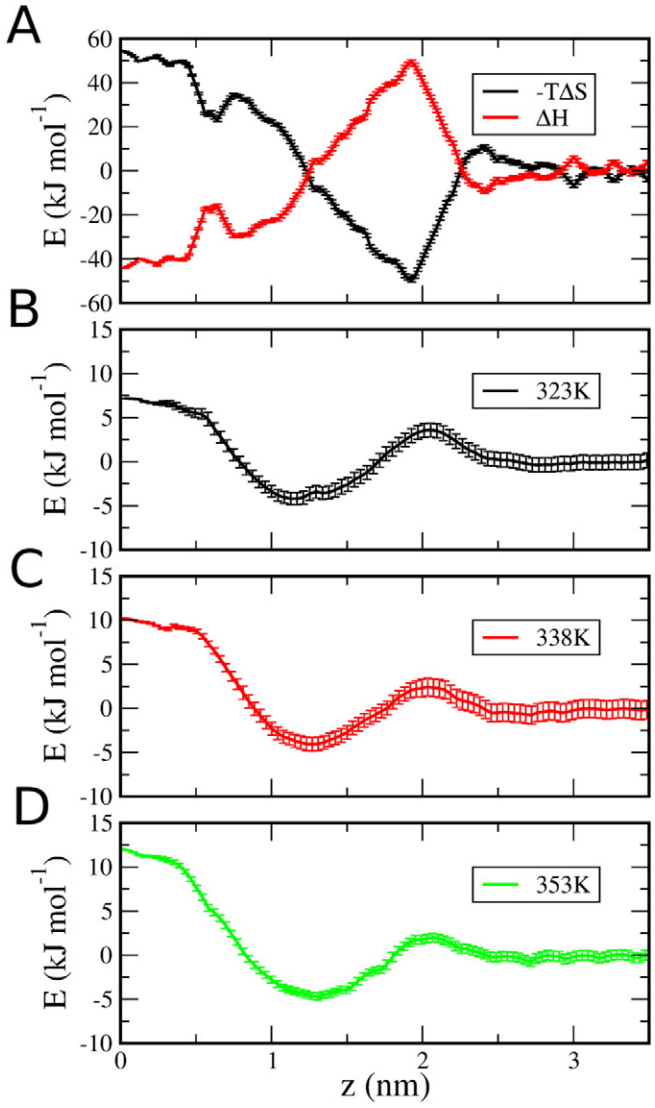

Fig. 2. Enthalpic and entropic contributions to PMF of MMTS–DPPC interaction. A) Free energy of a MMTS molecule from bulk water to a DPPC bilayer (black, entropic component of free energy, $-T\Delta S$; red, enthalpic component of free energy, ΔH). Temperature dependence of the free energy for transferring MMTS from water to a DPPC bilayer at B) 323 K (black), C) 338 K (red) and D) 353 K (green). Error bars were obtained by bootstrap analysis using g_wham.

compounds such as hexane, [28] amino acids [37], and non-steroidal drugs [38].

Fig. 2B-D shows the free energy of MMTS partition into a DPPC bilayer at three different temperatures. The three curves present similar shapes but small differences appear along the *z*-axis (Fig. 2B-D). Applying Eqs. (1) and (2), temperature dependence of free energy allowed us to calculate the spatially resolved enthalpy and entropy of the process (Fig. 2A). At around the region of the phosphate and choline groups, partitioning is favored by entropy, but opposed by enthalpy (Fig. 2A). Enthalpic contribution of MMTS partition into the lipid membrane at the lipid headgroup area presents positive values. As the MMTS moves from bulk to the interface, there is a maximal entropic contribution at 2 nm (head group region). The transfer of MMTS into the phosphate and choline groups region is driven by entropy increase probably due to the removal of water molecules solvating the hydrophobic portions of MMTS (hydrophobic effect) [39]. Unfavorable enthalpic term arises from the loss of H-bonding between water and MMTS.

MMTS partitioning into the upper region of the acyl chains, near the carbonyl group is driven by enthalpy but opposed by entropy (Fig. 2A). As we move deeper into the hydro carbonate chains of DPPC (1 to 0 nm), enthalpy contribution to MMTS partition becomes more favorable, that is it takes negative values (Fig. 2A). This enthalpy (ΔH) driven partition at the carbonyl region becomes stronger as MMTS penetrates into the acyl chains region due to favorable van der Waals interactions. Finally, enthalpy–entropy compensation is observed along the whole process (Fig. 2A). This is a general feature of processes that involve changes in hydrogen bonding [40].

MMTS interaction with C = O groups of the lipids is of relevance since carbonyls normal to the membrane constitute the first layer of dipoles on which water is polarized. These are important for structural transitions in PC lipids [41]. At MMTS: DPPC molar ratios higher than 0.75:1.00, a gradual increase of DPPC transition temperature is observed proportional to the MMTS concentration until a limit value of 53 °C is reached [1]. For the reasons exposed above, this interaction is expected to be relevant for the reported modification of DPPC bilayer transition temperature (Tm) with increasing concentrations of MMTS [1].

The cryoprotective agent dimethyl sulfoxide (DMSO), and MMTS are polar organosulfur compounds that can modify the Tm of lipids bilayers. In spite of their chemical similarities, DMSO is capable of modifying Tm of lipid bilayers in concentrations several times smaller than MMTS [42]. An analysis of DMSO partition into DPPC membranes and a direct comparison with that of MMTS could help to bring light into their mechanism of action. We performed PMF calculations of DMSO partition into DPPC bilayers to obtain the free energy profile at three different temperatures (323, 338 and 353 K) (Fig. 3B-D) and calculated the spatially resolved enthalpy and entropy of the process (Fig. 3A). Atomic charges employed for MMTS and DMSO molecules are shown in SM Fig. S-4. The ΔG of partition for DMSO in the membrane is positive, while for MMTS is negative in the upper region of the membrane. DMSO partitioning at the position of the polar head group as well as in the acyl chains is driven by entropy but opposed by enthalpy (Fig. 3).

When we analyzed MMTS and DMSO PMF profiles it can be seen that the first part of the PMF decomposition profile (from water to the DPPC headgroups) is similar for both molecules. However, there is none enthalpic partition of DMSO to any chemical region of DPPC. The release of water molecules could contribute to the gain of entropy observed for the partition of DMSO and MMTS in the upper region of DPPC bilayer (charge headgroups). A differential behavior of MMTS and DMSO is observed in the partition into the hydrocarbonate chains that is enthalpic for MMTS and entropic for DMSO.

3.3. All atom equilibrium MD simulations

In order to study and to describe the interaction of MMTS molecule and the DPPC membrane, MD runs of ~200 ns each were carried out with MMTS concentrations of ~0.088 M, ~0.18 M, ~0.33 M and ~0.44 adding 20, 40, 80 and 100 MMTS molecules located at random starting positions within 5 to 25 Å over the membrane plane (see Section 2). In order to corroborate the proper equilibration of the simulations the area per lipid (APL), density profiles and membrane thickness were evaluated (see SM, Figs. S-5.1 to S-5.3).

Fig. 4 shows the density profile during the last 100 ns simulation along the normal to the membrane plane (*z*-axis) of different DPPC membrane components, as well as MMTS molecules. The peak of MMTS density in the membrane is found in the region of the carbonyl groups of DPPC, whereas a valley was observed in the polar region of the phosphate and choline groups. This indicates that MMTS molecules are preferentially located in the region of the carbonyl groups (Fig. 4-B). Comparing the density plots of the MDs at different MMTS concentrations (from 0.088 to 0.44 M), a similar peak was found for the density of MMTS in the region of the carbonyls (see Fig. 4C and Fig. S-6 of the SM). This profile is consistent also with the free energy profile obtained from the PMF where the minimum energy for MMTS is located in the diglyceride region (Fig. 1). Integrating the area under the peak, and normalizing it to the number of molecules, we quantified MMTS molecules

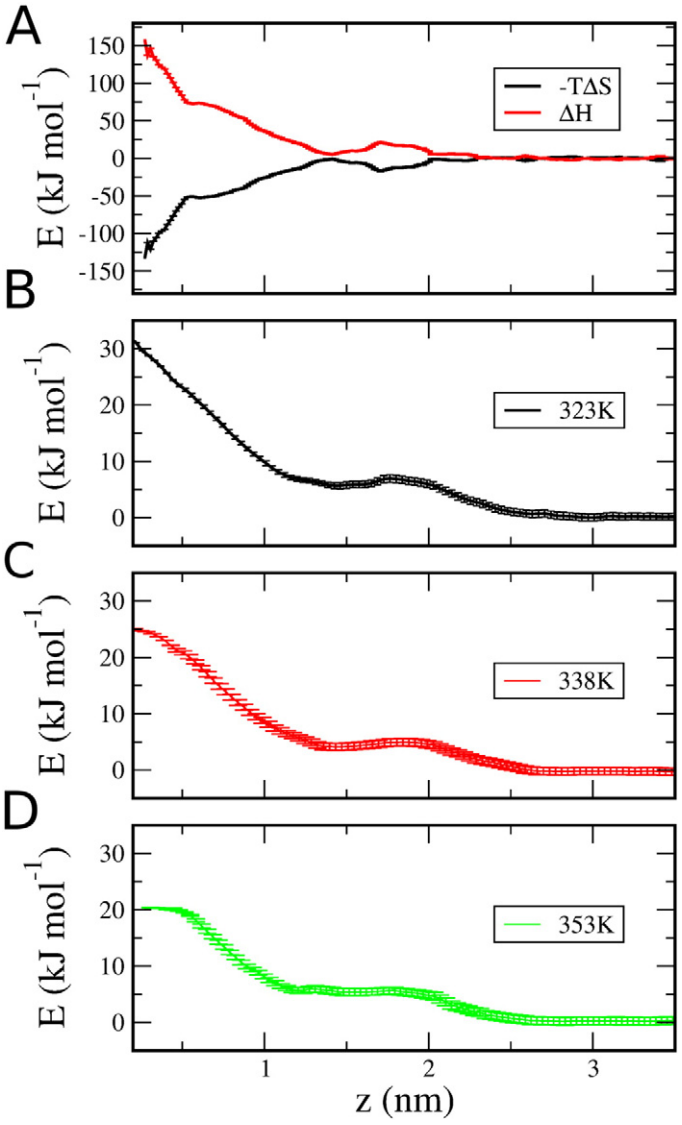

Fig. 3. Enthalpic and entropic contributions to PMF of DMSO-DPPC interaction. A) Free energy of partitioning a DMSO molecule from bulk water to a DPPC bilayer (black, entropic component of free energy, $-T\Delta S$; red, enthalpic component of free energy, ΔH). Temperature dependence of the free energy for transferring DMSO from water to a DPPC bilayer at B) 323 K (black), C) 338 K (red) and D) 353 K (green). Error bars were obtained by bootstrap analysis using g_wham.

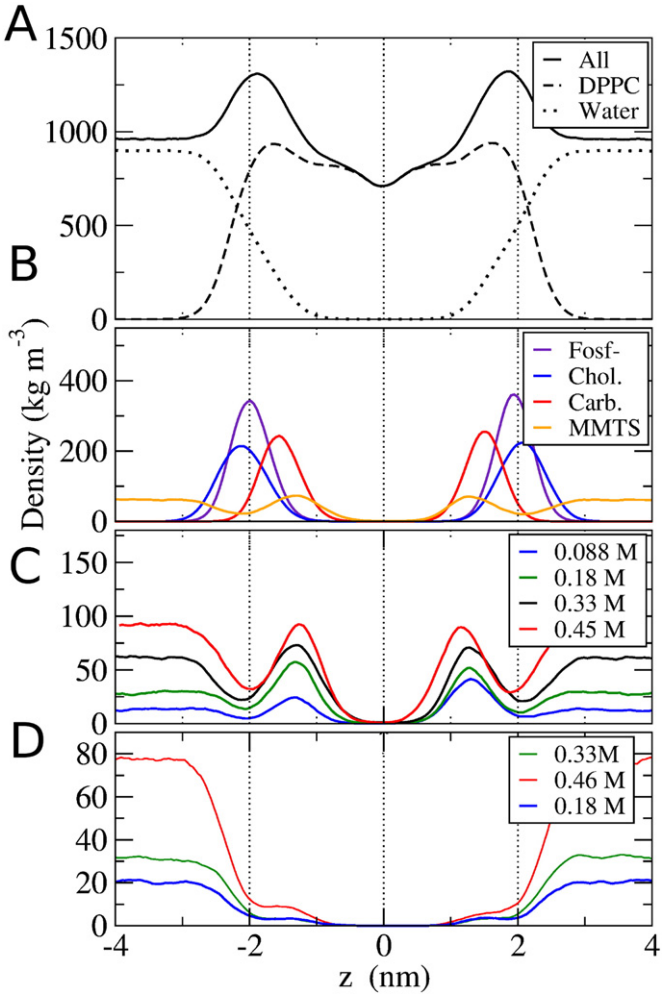

Fig. 4. Schematic diagrams of the density profile of the DPPC bilayer along the *z*-axis. The density profile of the whole system and relevant components of the system with 0.33 M of MMTS are shown in graphics A and B. The components are shown in different colors. A) Density profile of the whole system, DPPC and water in black. B) Choline groups in blue, carboxylic groups in red, phosphate groups in violet, and MMTS in orange. C) MMTS density profiles for the simulations at different MMTS concentrations. D) DMSO density profiles for the simulations at different MMTS concentrations.

located in the bilayer. The number varied from 10 to 36 molecules from the most diluted to the most concentrated solution (Fig. 4-C and Table S-2).

The degree of ordering of the acyl chains of the phospholipids can be determined from the deuterium order parameter (DOP), S_{CD} [43]. This parameter was employed to evaluate the effect of the interaction of MMTS with the membrane in the order of the acyl chains. Fig. 5 shows a comparison of the S_{CD} values at all concentrations analyzed of MMTS. It was found that the *sn*1 and *sn*2 chains (Scheme 1) were slightly affected by the presence of MMTS (Fig. 5). Two differential effects were observed. At low concentration, MMTS displayed a mild disordering effect, which vanished at higher concentrations (Fig. 5). A small ordering effect for the methylene groups closer to the carbonyl was observed for *sn1* chain at 0.33 and 0.44 M (Fig. 5A). This is in agreement with the preferred location of MMTS inside the bilayer according to MMTS ΔG of partition (Fig. 1) and density (Fig. 4C) profiles. These changes are related with an observed thinning of the membrane at low MMTS concentrations that vanished at higher concentrations (Table S-2), when the acyl chains became more ordered (Fig. 5).

The diffusion of MMTS from one side to the other of the bilayer was evaluated. In each MD, it was found that only 2 to 12 molecules crossed to the other side within 200 ns. This could also be observed in the density profile as an empty region in the center of the bilayer (Fig. 4C and D) (for a full list of the crossing molecules see supplementary material Figs. S-7.1 to S-7.4). A representative MMTS molecule diffusion process along the MD simulation is shown in Fig. 6. It can be observed that most of the time the MMTS molecule is inside the bilayer, it resides in the carbonyl region, while transmembrane crossing is a relatively fast event. We analyzed the chemical groups that interact when MMTS enters the bilayer following the variation of the minimum distance among these groups (Fig. S-8). This analysis showed that when MMTS enters the bilayer, CH_3 groups interact with carbonyl and in less extend with phosphate groups of DPPC. On the contrary S = O moiety does not interact with any DPPC functional groups.

The sequence of MMTS translocation through the membrane is represented in the five selected frames included in Fig. 7. In general, it was observed that the crossing occurred in two steps; in the first step the molecule reach the center of the bilayer, stabilized by another MMTS molecule or by water molecules. Then, after some of picoseconds, the MMTS molecule is picked up by a molecule located in the transmembrane region (another MMTS molecule, a lipid or eventually by some

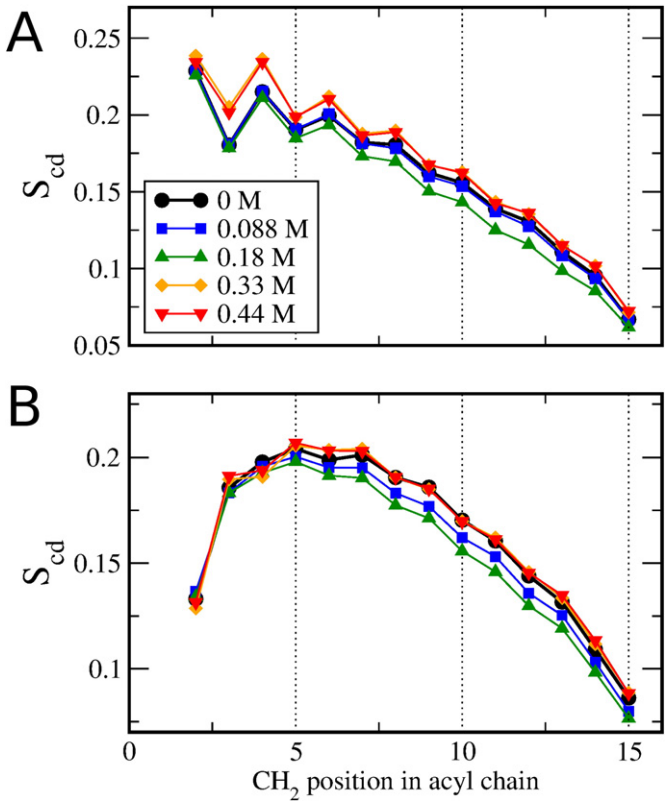

Fig. 5. Profile of the MMTS effects on the deuterium order parameters (S_{CD}) of DPPC acyl chains for (A) *sn*1 chain (B) *sn*2 chain.

water molecules in the region of 7 to 10 Å from the center of the bilayer). Subsequently, it rapidly moves to the carbonyls region were could be stabilized by means of H-bond with the C=O groups of the lipids. As observed with DMSO and other cryoprotective compounds, MMTS molecule could act as a water carrier when crossing the membrane. However, for the few MMTS molecules that permeated the membrane during the simulations, no pore formation or water transport to the other side of the membrane were observed. This is reflected in the graphics of the number of atoms from and/or MMTS molecules in the

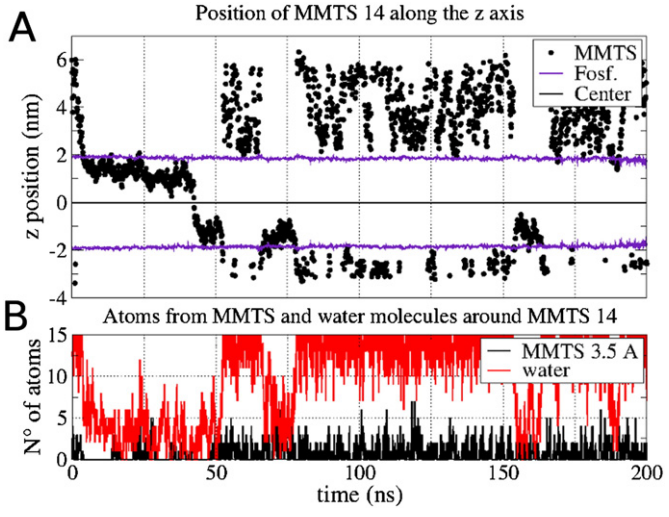

Fig. 6. A) Distribution of an MMTS molecule along the *z*-axis, normal to the bilayer, during the simulation. In details are represented the position of the functional groups of the DPPC. B) Representation of the number of number of atoms from water and MMTS molecules (black) at 3.5 Å around the MMTS studied molecule.

proximity of the crossing molecule, which is zero when the MMTS is crossing to the other side, at 40 to 45 ns (Fig. 6). Also, when the total number of hydrogen bonds of MMTS molecules with water was analyzed, a reduction associated with MMTS insertion into the bilayer was observed (see Fig. S-9 of SM). For every MMTS molecule that enters the bilayer, two molecules of MMTS waters shell are lost.

With the aim of comparing MMTS and DMSO mode of action, we ran 200 ns MD simulations of three DMSO concentrations of ~0.18 M, ~0.36 M and ~0.45 M adding 40, 80 and 100 DMSO molecules, respectively. In order to corroborate the proper equilibration of the simulations, the area per lipid (APL), density profiles and membrane thickness and DOP were also evaluated, as for MMTS (see Fig. S-10.1 to S-10.3-9 and Table S-3 of SM). Density profiles obtained during the last 100 ns indicate that most of DMSO molecules remain in water solution (Fig. 4D). This profile is also consistent with the free energy profile obtained from the PMF where the energy for DMSO partition into membrane is positive (Fig. 3).

We quantified DMSO molecules located in the bilayer and found that 2, 4 and 8 molecules were located inside the membrane for ~0.18, ~0.36 and ~0.45, respectively (see Fig. 4-D and Table S-3 of SM). The diffusion of DMSO from one side to the other of the bilayer was evaluated. In each MD, it was found that unlike MMTS, no DMSO molecules crossed to the other side within the time analyzed (see Fig. 8 and S-11), what is more they do not even reach the center of the bilayer. At the concentrations analyzed, DMSO had no effect on S_{CD} parameter (Fig. S-12, SM). Leekumjorn and Sum analyzed the diffusion process of DMSO at similar concentrations as the one used in this work using a UA model [39]. They found that 9 of 96 DMSO molecules were able to diffuse trough the bilayer and reach the opposite aqueous phase [39]. In agreement with our results Leekumjorn and Sum found that deuterium order parameters for the lipid tails of DPPC were not affected at this DMSO concentration [39]. These results contrast with the order parameter profiles obtained in presence of DMSO using GROMOS $53A6_L$ force field [44], that showed that DMSO interaction with the membrane causes the acyl chains to became disordered and that it induced pore formation [44]. Nevertheless, concentrations used in these simulations were at least ten times higher [44].

3.4. Coarse grained free diffusion MD simulations

Coarse-grained (CG) models offer the possibility to analyze processes that occur at long length/time scales. The most commonly used CG force field for lipids is the MARTINI FF [33]. The MARTINI model is based on a four-to-one mapping, where an average of four heavy atoms and its associated hydrogens are represented by a single bead or interaction center [33]. Water CG models group several water molecules (3 or 4) into a single unit. A water model that provides a good representation of the electrostatic interaction has been developed by Wu et al. [31] the so-called Big Multi-pole Water (BMW) model [31]. This model is compatible with the MARTINI FF [33]. Since coarse-graining modifies the energy landscape to become smoother, effective simulation times are larger. In the case of Martini, the time scale is approx. 4 times the formal simulation length [45]. Taking this into account, and in order to achieve longer MD times, we used BMW FF to parameterize a CG MMTS model (see Methods section). We calculated membrane partition profiles of different CG models of MMTS and compare it with the AA profile obtained above (Fig. S-3). We obtained a simplified model of MMTS that consists of two CG beads, C5 and Na (using the same denomination as reference [33]). C5 beads represent the nonpolar groups while the Na bead is a hydrogen bond acceptor that represents the H-bonding atoms of MMTS (S=0). As it can be observed in Fig. S-3, the two-bead MMTS CG model presents a very similar PMF profile to that of the AA model. With this model, we performed CG MMTS free diffusion MD simulations using a pre-equilibrated 128 DPPC lipid bilayer downloaded from BMW-Martini developer's homepage [34] in the presence of 96 MMTS molecules (0.42 M). We ran 2 μs (~8 μs of

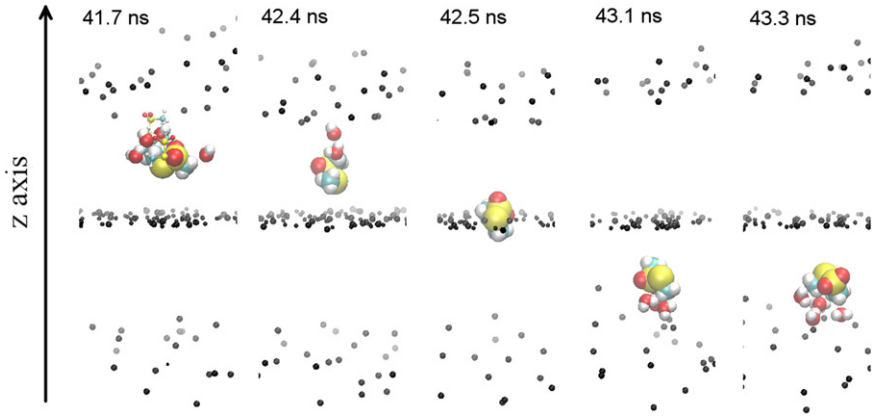

Fig. 7. Selected five frames from one of the three DPPC-MMTS simulations. These specific frames were used to shown how an MMTS molecule percolates the bilayer.

effective time) MD simulations and analyzed MMTS effect onto DPPC bilayer.

It was observed that after 70 ns (~300 ns of effective time) all MMTS molecules were inside the membrane. This is reflected in the density profile (Fig. 9). The MMTS density profile peak matches that of the GL beads that correspond to the DPPC glycerol group (see supplementary Scheme S-1). This is in accordance with the PMF profile obtained during MMTS CG parameterization. Although in the CG models such as Martini the balance between enthalpy and entropy is affected, Martini is parameterized to reproduce accurate free energies [45]. As observed in Fig. S-3, we were able to reproduce the AA PMF profile of MMTS partition into the membrane quite well. It should be taken into account that CG models present some limitations at a fundamental level such as kinetics that are modified in unpredictable ways [45]. This should be corrected extending the sampling time. We performed two replicas of 2 μs each, but we could not reproduce the MMTS density profile obtained with the AA force field. Taking these considerations into account, the results of these CG simulations should be interpreted with care.

We calculated the order parameter (P2) for DPPC using the do_order script [46] that calculates the angle between the bond of different beads and the normal to the bilayer plane. A P2 value of 0 indicates random orientation while P2 = 1 indicates a perfect alignment with the bilayer normal. A DPPC bilayer free of MMTS was used as a reference. In Fig. 10 the order parameters of a DPPC bilayer in presence (black) or in absence (red) of MMTS is showed. It can be observed that MMTS molecules exerted an ordering effect onto GL–C1 bond (Fig. 10). This is in agreement with the results obtained with the AA MD, where an ordering effect was observed at high concentrations in the methylene groups nearer the carbonyl (Fig. 5). Also, the effect was slightly higher for GL2–C1B bond (Fig. 10), which corresponds to the *sn1* chain of AA DPPC (Fig. 5).

Unlike previous CG MD simulations of DMSO [47] no water pore formation was observed even when the number of molecules was doubled (192 DMSO) (data not shown). This is another evidence of the differences in the MMTS and DSMO interactions with DPPC membranes. However, we should mention that experimentally, permeability enhancement occurs at DMSO concentrations higher than 26 mol% almost ten times higher than the ones used in this work. Experimentally, permeability enhancement occurs at DMSO concentrations higher than 26 mol%. [48].

4. Conclusions

In the present work we performed MD simulations of lipid bilayers in the presence of the protective agent MMTS in order to contribute to the characterization of its mode of action by determining its binding site and its diffusional properties. These results were contrasted with

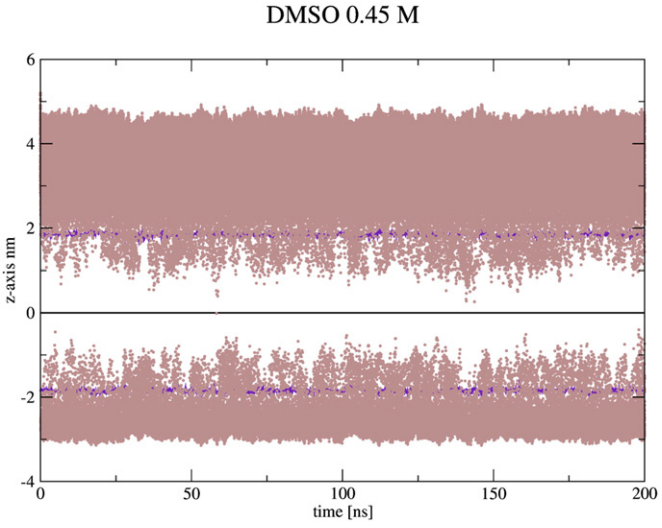

Fig. 8. Position of the center of mass, along the *z*-axis, of all the DMSO molecules during all time of the simulation, for the solution with [DMSO] = 0.45 M.

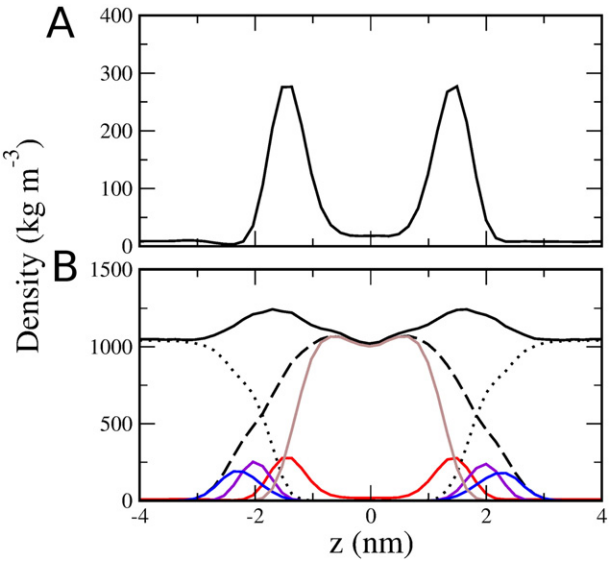

Fig. 9. Density profile of the CG MD simulation system along the *z*-axis. The density profile of the whole system and relevant components of the system with 0.42 M of CG MMTS are shown in graphics A and B. A) CG MMTS density profile. B) Choline bead in blue, the glycerol bead in red, the phosphate bead in violet, and carbon beads in brown. C).

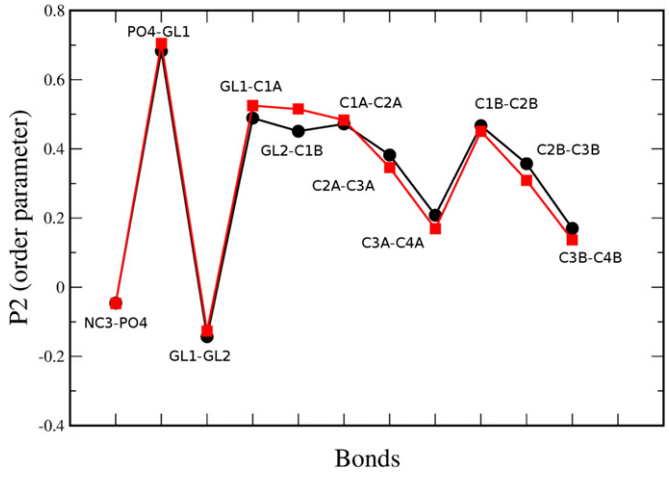

Fig. 10. Order parameter (P2) for CG DPPC. C1A–C4A are the beads of the hydrocarbon chain A, while C1B–C4B correspond to Chain B. (see scheme in Fig. S-2).

the ones obtained for the chemically related cryoprotective agent DMSO.

PMF profile showed a favorable partition of MMTS to the membrane ($\Delta G_{partition} \sim -5$ KJ·mol^{-1}). For DMSO instead no favorable partition in the membrane was found ($\Delta G_{partition} \sim 7.5$ KJ·mol^{-1}). PMF profile decomposition to obtain the enthalpic and entropic contributions of the $\Delta G_{partition,}$ showed that MMTS presents and enthalpic partition caused by a specific interaction of this compound with the carbonyl region of phospholipid acyl chain. This effect was not observed for DMSO with a really different profile where the partition is driven by entropy.

The results of the simulations are in agreement with previous experimental results where an interaction between the MMTS molecule and the carbonyl groups of the DPPC bilayer was found [1]. The analysis of free diffusion MD simulations allowed us to gained information on the diffusional properties of both compounds.

Our results support the idea that MMTS ΔG for binding receives favorable entropy contribution because the hydrophobic parts of the molecule are removed from water. Water molecules previously in the hydration phase of MMTS are released to the bulk phase. This characteristic would be shared with DMSO. On the other hand, differences arise once inside the membrane, where a favorable interaction of MMTS with DPPC helps to establish the minimum in the carbonyl region. The differential interactions with the hydrocarbonated chain of lipids suggest a difference between these two compounds. Finally, according to the results presented in here we found that the mechanisms by which DMSO and MMTS shift the Tm could be different due to the differential effects of DMSO and MMTS on the membrane properties.

Transparency document

The Transparency document associated with this article can be found online.

Acknowledgments

This work was supported in part by the Consejo Nacional de Investigaciones Científicas y Tecnológicas (CONICET), the Agencia Nacional de Promoción Científica y Tecnológica (FONCYT, Argentina), the Agencia Córdoba Ciencia and the Secretaría de Ciencia y Técnica (SECYT) of the Universidad Nacional de Córdoba. INFIQC and INQUINOA are jointly sponsored by CONICET and the universities Universidad Nacional de Córdoba and Universidad Nacional de Tucumán. All calculations were performed with computational resources from CCAD-Universidad Nacional de Córdoba (http://ccad.unc.edu.ar/), in particular the Cristina supercomputer, built through an ANPCYT special funding (grant PME-2006-01581) and the Mendieta Cluster that belongs to the Facultad de Matemática, Astronomía y Física, that is also part of SNCAD-MinCyT, República Argentina. E.D.L. gratefully acknowledges the receipt of a PhD fellowship from CONICET.

Appendix A. Supplementary data

Supplementary data to this article can be found online at http://dx.doi.org/10.1016/j.bbamem.2015.10.008.

References

[1] M.E. Defonsi Lestard, S.B. Diaz, M.E. Tuttolomondo, S. Sanchez Cortez, M. Puiatti, A.B. Pierini, A. Ben Altabef, Interaction of S-methyl methanethiosulfonate with DPPC bilayer, Spectrochimica Acta. Part A, Molecular and biomolecular spectroscopy 97 (2012) 479–489.
[2] M.I. Gurr, J.L. Harwood, K.N. Frayn, Lipid Biochemistry: An Introduction, 5th ed., 2002 320.
[3] N. Ridgway, R. McLeod, J.E. Vance, D. Vance, *Biochemistry of Lipids, Lipoproteins and Membranes* (2008) 624.
[4] S. Samanta, S. Hezaveh, G. Milano, D. Roccatano, Diffusion of 1,2-dimethoxyethane and 1,2-dimethoxypropane through phosphatidycholine bilayers: a molecular dynamics study, J. Phys. Chem. B 116 (2012) 5141–5151.
[5] E.H. Hill, K. Stratton, D.G. Whitten, D.G. Evans, Molecular dynamics simulation study of the interaction of cationic biocides with lipid bilayers: aggregation effects and bilayer damage, Langmuir 28 (2012) 14849–14854.
[6] J.L. MacCallum, W.F. Bennett, D.P. Tieleman, Transfer of arginine into lipid bilayers is nonadditive, *Biophys. J. 101* (**2011**) 110–117.
[7] M.A. Villarreal, M. Perduca, H.L. Monaco, G.G. Montich, Binding and interactions of L-BABP to lipid membranes studied by molecular dynamic simulations, Biochim. et Biophys. Acta 2008 (1778) 1390–1397.
[8] J.B. Klauda, R.M. Venable, J.A. Freites, J.W. O'Connor, D.J. Tobias, C. Mondragon-Ramirez, I. Vorobyov, A.D. MacKerell Jr., R.W. Pastor, Update of the CHARMM all-atom additive force field for lipids: validation on six lipid types, J. Phys. Chem. B 114 (2010) 7830–7843.
[9] C.J. Dickson, B.D. Madej, A.A. Skjevik, R.M. Betz, K. Teigen, I.R. Gould, R.C. Walker, Lipid14: the amber lipid force field, J. Chem. Theory Comput. 10 (2014) 865–879.
[10] J.P. Jämbeck, A.P. Lyubartsev, Implicit inclusion of atomic polarization in modeling of partitioning between water and lipid bilayers, Phys. Chem. Chem. Phys. 15 (2013) 4677–4686.
[11] (a) J. Wang, R.M. Wolf, J.W. Caldwell, P.A. Kollman, D.A. Case, Development and testing of a general amber force field, J. Comput. Chem. 25 (2004) 1157–1174;
(b) J. Wang, P. Cieplak, P.A. Kollman, How well does a restrained electrostatic potential (RESP) model perform in calculating conformational energies of organic and biological molecules? J. Comput. Chem 21 (2000) 1049–1074.
[12] Y. Nakamura, T. Matsuo, K. Shimoi, I. Tomita, S-methyl methane thiosulfonate, a new antimutagenic compound isolated from *Brassica oleracea* L. var. botrytis, Biol. Pharm. Bull 16 (1993) 207–209.
[13] S. Sugie, K. Okamoto, M. Ohnishi, H. Makita, T. Kawamori, T. Watanabe, T. Tanaka, Y.K. Nakamura, Y. Nakamura, I. Tomita, H. Mori, Suppressive effects of S-methyl methanethiosulfonate on promotion stage of diethylnitrosamine-initiated and phenobarbital-promoted hepatocarcinogenesis model, *Jap. J. Cancer Res.: Gann* 88 (1997) 5–11.
[14] (a) M.A. Villarreal, S.B. Diaz, E.A. Disalvo, G.G. Montich, Molecular dynamics simulation study of the interaction of trehalose with lipid membranes, Langmuir *20* (2004) 7844–7851;
(b) C.J. Garvey, T. Lenne, K.L. Koster, B. Kent, G. Bryant, Phospholipid membrane protection by sugar molecules during dehydration—insights into molecular mechanisms using scattering techniques, Int. J. Mol. Sciences 14 (2013) 8148–8163.
[15] (a) P. Westh, Preferential interaction of dimethyl sulfoxide and phosphatidyl choline membranes, Biochim. Biophys. Acta 1664 (2004) 217–223;
(b) A.A. Gurtovenko, J. Anwar, Modulating the structure and properties of cell membranes: the molecular mechanism of action of dimethyl sulfoxide, J. Phys. Chem. B 111 (2007) 10453–10460.
[16] Y.H. Yoon, J.M. Pope, J. Wolfe, The effects of solutes on the freezing properties of and hydration forces in lipid lamellar phases, Biophys. J. 74 (1998) 1949–1965.
[17] B. Hess, C. Kutzner, D. van der Spoel, E. Lindahl, GROMACS 4: algorithms for highly efficient, load-balanced, and scalable molecular simulation, J. Chem. Theory Comput 4 (2008) 435–447.
[18] J.P. Jambeck, A.P. Lyubartsev, Derivation and systematic validation of a refined all-atom force field for phosphatidylcholine lipids, J. Phys. Chem. B 116 (2012) 3164–3179.
[19] W.L. Jorgensen, J. Chandrasekhar, J.D. Madura, R.W. Impey, M.L. Klein, Comparison of simple potential functions for simulating liquid water, J. Chem. Phys. 79 (1983) 926.
[20] http://mmkluster.fos.su.se/slipids/. Accessed date 21 July, 2015
[21] C.I. Bayly, P. Cieplak, W. Cornell, P.A. Kollman, A well-behaved electrostatic potential based method using charge restraints for deriving atomic charges: the RESP model, J. Phys. Chem. 97 (1993) 10269–10280.
[22] M.J.T. Frisch, G. W ., H.B. Schlegel, G.E. Scuseria, M.A. Robb, J.R. Cheeseman, J.A. Montgomery Jr., T. Vreven, K.N. Kudin, J.C. Burant, J.M. Millam, S.S. Iyengar, J. Tomasi, V. Barone, B. Mennucci, M. Cossi, G. Scalmani, N. Rega, G.A. Petersson, H. Nakatsuji, M. Hada, M. Ehara, K. Toyota, R. Fukuda, J. Hasegawa, M. Ishida, T. Nakajima, Y.

Honda, O. Kitao, H. Nakai, M. Klene, X. Li, J.E. Knox, H.P. Hratchian, J.B. Cross, V. Bakken, C. Adamo, J. Jaramillo, R. Gomperts, R.E. Stratmann, O. Yazyev, A.J. Austin, R. Cammi, C. Pomelli, J.W. Ochterski, P.Y. Ayala, K. Morokuma, G.A. Voth, P. Salvador, J.J. Dannenberg, V.G. Zakrzewski, S. Dapprich, A.D. Daniels, M.C. Strain, O. Farkas, D.K. Malick, A.D. Rabuck, K. Raghavachari, J.B. Foresman, J.V. Ortiz, Q. Cui, A.G. Baboul, S. Clifford, J. Cioslowski, B.B. Stefanov, G. Liu, A. Liashenko, P. Piskorz, I. Komaromi, R.L. Martin, D.J. Fox, T. Keith, M.A. Al-Laham, C.Y. Peng, A. Nanayakkara, M. Challacombe, P.M.W. Gill, B. Johnson, W. Chen, M.W. Wong, C. Gonzalez, J.A. Pople, *Gaussian 03, Revision C.02*, Revision C.022004.

[23] T. Fox, P.A. Kollman, Application of the RESP Methodology in the Parametrization of Organic Solvents, J. Phys. Chem. B 102 (1998) 8070–8079.

[24] A.W. Sousa da Silva, W.F. Vranken, ACPYPE - AnteChamber PYthon Parser interfacE, BMC Res. Notes 5 (2012) 367.

[25] M.E. Tuttolomondo, A. Navarro, T.P. Ruiz, E.L. Varetti, S.A. Hayes, D.A. Wann, H.E. Robertson, D.W. Rankin, A.B. Altabef, Gas-phase structure, rotational barrier, and vibrational properties of methyl methanethiosulfonate, CH3SO2SCH3: an experimental and computational study, J. Phys. Chem. A 111 (2007) 9952–9960.

[26] S. Kumar, J.M. Rosenberg, D. Bouzida, R.H. Swendsen, P.A. Kollman, THE weighted histogram analysis method for free-energy calculations on biomolecules. I. The method, *J. Comput. Chem.* 13 (1992) 1011–1021.

[27] J.S. Hub, B.L. de Groot, D. van der Spoel, g_wham—a free weighted histogram analysis implementation including robust error and autocorrelation estimates, J. Chem. Theory Comput 6 (2010) 3713–3720.

[28] J.L. MacCallum, D.P. Tieleman, Computer simulation of the distribution of hexane in a lipid bilayer: spatially resolved free energy, entropy, and enthalpy profiles, J. Am. Chem. Soc. 128 (2006) 125–130.

[29] http://mmkluster.fos.su.se/slipids/Downloads.html/. Accesed date 5 August, 2015

[30] U. Essmann, L. Perera, M.L. Berkowitz, T. Darden, H. Lee, L.G. Pedersen, A smooth particle mesh Ewald method, J. Chem. Phys. 103 (1995) 8577.

[31] Z. Wu, Q. Cui, A. Yethiraj, A new coarse-grained model for water: the importance of electrostatic interactions, J. Phys. Chem. B 114 (2010) 10524–10529.

[32] http://md.chem.rug.nl/cgmartini/index.php/parametrzining-new-molecule. Accesed date 5 August, 2015

[33] S.J. Marrink, H.J. Risselada, S. Yefimov, D.P. Tieleman, A.A.H. de Vries, The MARTINI force field: coarse grained model for biomolecular simulations, J. Phys. Chem. B 111 (2007) 7812–7824.

[34] http://yethiraj.chem.wisc.edu/downloads. Acces date August 5, 2015

[35] http://md.chem.rug.nl/cgmartini/index.php/tools22015.

[36] J.F. Nagle, S. Tristram-Nagle, Structure of lipid bilayers, Biochim. Biophys. Acta 1469 (2000) 159–195.

[37] J.L. MacCallum, W.F. Bennett, D.P. Tieleman, Distribution of amino acids in a lipid bilayer from computer simulations, Biophys. J. 94 (2008) 3393–3404.

[38] M.B. Boggara, R. Krishnamoorti, Partitioning of nonsteroidal antiinflammatory drugs in lipid membranes: a molecular dynamics simulation study, Biophys. J. 98 (2010) 586–595.

[39] S. Leekumjorn, A.K. Sum, Molecular study of the diffusional process of DMSO in double lipid bilayers, Biochim. Biophys. Acta 2006 (1758) 1751–1758.

[40] E.A. Disalvo, M.F. Martini, A.M. Bouchet, A. Hollmann, M.A. Frias, Structural and thermodynamic properties of water-membrane interphases: significance for peptide/membrane interactions, Advances Colloid and Interface Science 211 (2014) 17–33.

[41] E. Disalvo, F. Lairion, F. Martini, H. Almaleck, S. Diaz, G. Gordillo, Water in biological membranes at interfaces: does it play a functional role, J. Argent. Chem. Soc. 92 (2004) 1–22.

[42] A.P. Dabkowska, L.E. Collins, D.J. Barlow, R. Barker, S.E. McLain, M.J. Lawrence, C.D. Lorenz, Modulation of dipalmitoylphosphatidylcholine monolayers by dimethyl sulfoxide, Langmuir 30 (2014) 8803–8811.

[43] A. Seelig, J. Seelig, The dynamic structure of fatty acyl chains in a phospholipid bilayer measured by deuterium magnetic resonance, Biochemistry 13 (1974) 4839–4845.

[44] Z.E. Hughes, A.E. Mark, R.L. Mancera, Molecular dynamics simulations of the interactions of DMSO with DPPC and DOPC phospholipid membranes, J. Phys. Chem. B 116 (2012) 11,911–11,923.

[45] S.J. Marrink, D.P. Tieleman, Perspective on the Martini model, Chem. Soc. Rev. 42 (2013) 6801–6822.

[46] http://md.chem.rug.nl/cgmartini/index.php/tools2. Accesed date 5 August, 2015

[47] R. Notman, M. Noro, B. O'Malley, J. Anwar, Molecular basis for dimethylsulfoxide (DMSO) action on lipid membranes, Journal of the American Chemical Society 128 (43) (2006) 13,982–13,983.

[48] A.C. Williams, B.W. Barry, Penetration enhancers, Advanced drug delivery reviews 56 (5) (2004) 603–618.